Non-destructive evaluation, inspection and testing of primary aeronautical composite structures using phase contrast X-Ray imaging

NON-DESTRUCTIVE EVALUATION, INSPECTION AND TESTING OF PRIMARY AERONAUTICAL COMPOSITE STRUCTURES USING PHASE CONTRAST X-RAY IMAGING

VINCENT REVOL[*], THOMAS STADELMANN

Robotics & Packaging, CSEM SA, Untere Gründlistrasse 1,
Alpnach Dorf 6055,Switzerland
vincent.revol@csem.ch[†]
http://www.csem.ch

KONSTANTINOS KITSIANOS, MARC-OLIVIER SAUER, ILIAS KOULALIS, ROLAND CHEMAMA

GMI Aero, 9 rue Buffault,
Paris 75009, France
konstantinos.kitsianos@gmi-aero.com
http://www.gmi-aero.com/

MATTHIEU GRÉSIL

School of Materials, The University of Manchester, Paper Science Building-E1C
Manchester M13 9PL, United Kingdom
matthieu.gresil@manchester.ac.uk
http://www.materials.manchester.ac.uk/

HERVÉ TRÉTOUT

Centre de Développement Exploratoire (DDPP/CDE), Dassault Aviation, 1 avenue du Parc
Argenteuil, 95100, France
Herve.Tretout@dassault-aviation.com
http://www.dassault-aviation.com/

GEORGES KANDERAKIS

Faculty of Applied Sciences, National Technical University of Athens, Ir. Politechniou 9
Kesariani 161 21, Greece
gkandera@central.ntua.gr
http://www.ntua.gr

ANA-MARIA MADRIGAL

Marketing & Business Development, CSEM SA, 1 rue Jaquet-Droz,
Neuchâtel 2002,Switzerland
anamaria.madrigal@csem.ch
http://www.csem.ch

Abstract

The EU-project EVITA (non-destructive EValuation, Inspection and Testing of primary Aeronautical composite structures using phase contrast X-ray imaging) aims at bringing Grating-based Phase Contrast X-ray imaging technology to non-destructive evaluation and inspection of primary and/or complex and thick aeronautical composite structures. In this article, the demonstrator built within the project will be presented as well as the results of the experimental study performed on aeronautical composite test samples.

Keywords Non-destructive inspection; composite materials; x-ray phase contrast imaging; grating interferometry

1. Introduction

Grating-based Phase Contrast X-Ray Imaging is based on the so-called Talbot-Lau interferometer, which is made of the combination of a standard X-ray apparatus with three transmission gratings as documented in the literature (David et al. 2002; Momose et al. 2003; Pfeiffer et al. 2006; Revol et al. 2010).

The method derives its potential from the fact that three different contrast mechanisms are combined in a single measurement. Indeed, not only the conventional absorption image can be extracted but also the refraction image

(also called differential phase contrast image) and the scattering image (also called dark field image), which are related respectively to the refraction of the X-ray beam inside the sample and to the ultra-small angle scattering caused by its microstructure. Preliminary studies have shown that the scattering image provides a powerful tool to detect any change in the arrangement of the fibers due to the presence of defects such as porosity, fiber waviness, micro-cracks or resin rich/resin poor areas (Revol et al. 2013; Revol et al. 2012; Jerjen et al. 2013; Kottler et al. 2012).

Within the project EVITA (www.evita-project.eu), the requirements and needs of the aeronautics industry in terms of the non-destructive inspection of thick and thin composite components were collected and analyzed. From there, a customized demonstrator was designed and realized in order to benchmark this novel technology against the following non-destructive inspection (NDI) techniques: water jet ultrasonic, phased array ultrasonic, thermography and computed tomography.

2. Phase Contrast X-Ray Imaging

A schematic view of the grating-based Phase Contrast X-Ray Imaging system is shown in Figure 1. It consists of a standard high power X-ray source (Varian HPW-160-11) and pixelated detector array (Dexela DEX2315) coupled to three gratings forming an X-ray interferometer. The principle of the X-ray grating interferometer is explained in details in the literature (David et al. 2002; Momose et al. 2003; Weitkamp et al. 2005; Pfeiffer et al. 2006).
A collimator made out of lead is used to control the illuminated area while a shutter allows to block the X-ray beam during the idle time of the detector. In the present configuration, the sample can be moved independently using an XY gantry (IAI axis).

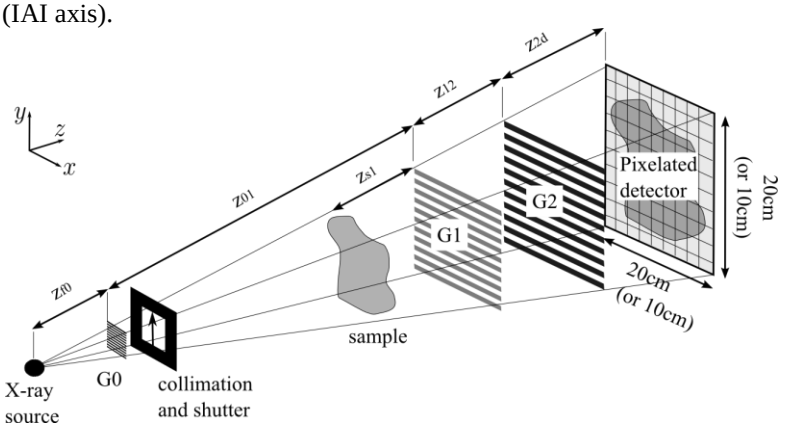

Figure 1. Schematic view of the grating-based Phase Contrast X-Ray Imaging system

The gratings were manufactured at CSEM using MEMS fabrication processes on Silicon wafers of diameter 150mm, which allows to achieve a grating size of 100×100mm on a single wafer.

The parameters of the demonstrator are summarized in Table 1.

	Parameters
Source acceleration voltage	40 – 70 kV
Maximal sample thickness (CFRP)	50 mm
System length (source to detector)	1.45 m
Measurement area (stitching mode)	1× 0.5 m^2
Image size (single field)	7 × 7 cm^2
Effective pixel size	50 - 60 µm

Table 1. Key parameters of the EVITA demonstrator

Three images are obtained using the EVITA demonstrator, namely the absorption, refraction and scattering images. The absorption image corresponds to the conventional X-ray image, except that the blurring effect due to the Compton scattering is suppressed in the direction perpendicular to the grating lines. The absorption image is related to the attenuation coefficient of the material and its thickness.

The refraction image is proportional to the refraction angle measured pixel-wise by the interferometer. The refraction angle is linked to the derivative of the phase shift in the direction perpendicular to the grating lines (direction y in Figure 1). In contrast to the absorption image, the refraction image is thus related to the refraction coefficient as well as to the thickness of the sample (Revol et al. 2010).

Finally, the scattering image is related to the ultra-small angle X-ray scattering (USAXS) of the beam inside the sample. It has been shown that the USAXS can be expressed in terms of variations of the electronic density of the material at the microscopic level (Yashiro et al. 2010). The scattering image is thus a perfect tool to probe the microscopic texture of composite materials and detect porosity, cracks and variations of the fibre density or orientation (Revol et al. 2011).

The images were reconstructed using the phase stepping method (Weitkamp et al. 2005), where the phase stepping was achieved by translation of the grating G2. The X-ray tube source was set to the small focal spot ($0.4\times0.4mm^2$) with the acceleration voltage at 60kVp and the anode current at 10mA. 19 phase steps were acquired over 4 periods with an individual exposure time of 750ms. The measurement was repeated 4 times and averaged. The measurement time for a single field inclusive reconstruction amounts to about 60s.

3. Results

The demonstrator was assembled in the premises of CSEM in Alpnach, Switzerland (see Figure 2) and started operation in January 2015. It was evaluated using coupon samples with different artificially prepared flaws. The samples were made out of Epoxy-carbon prepreg (HexPly 914C-T300H(6K)-5-34%). The results presented here were obtained with a 32 plies quasi-isotropic lay-up (+45°/90°/-45°/0°)4s with a thickness of about 4mm.

The results obtained with the EVITA demonstrator were benchmarked against four state-of-the-art NDI methods: water jet ultrasonic, phased array ultrasonic, thermography and computed tomography. The benchmarking measurements were performed at the University of Manchester, United Kingdom.

Figure 2. Picture of the EVITA demonstrator at CSEM in Alpnach, Switzerland. The demonstrator is operational since January 2015 and is acquiring data since then.

Figure 3 shows the results of the comparison for the first sample, where the mid-plane ply was cut across the width of the laminate perpendicular to the 0° direction. The spacing between the cut fibre ends amounts to 8mm, 4mm, 2mm, 1mm, 0mm (see Figure 3-a). The cut fibres can be detected in the scattering image (red arrows)

using the EVITA demonstrator as well as with the phased array system. All other benchmarking methods were not able to detect the defects.

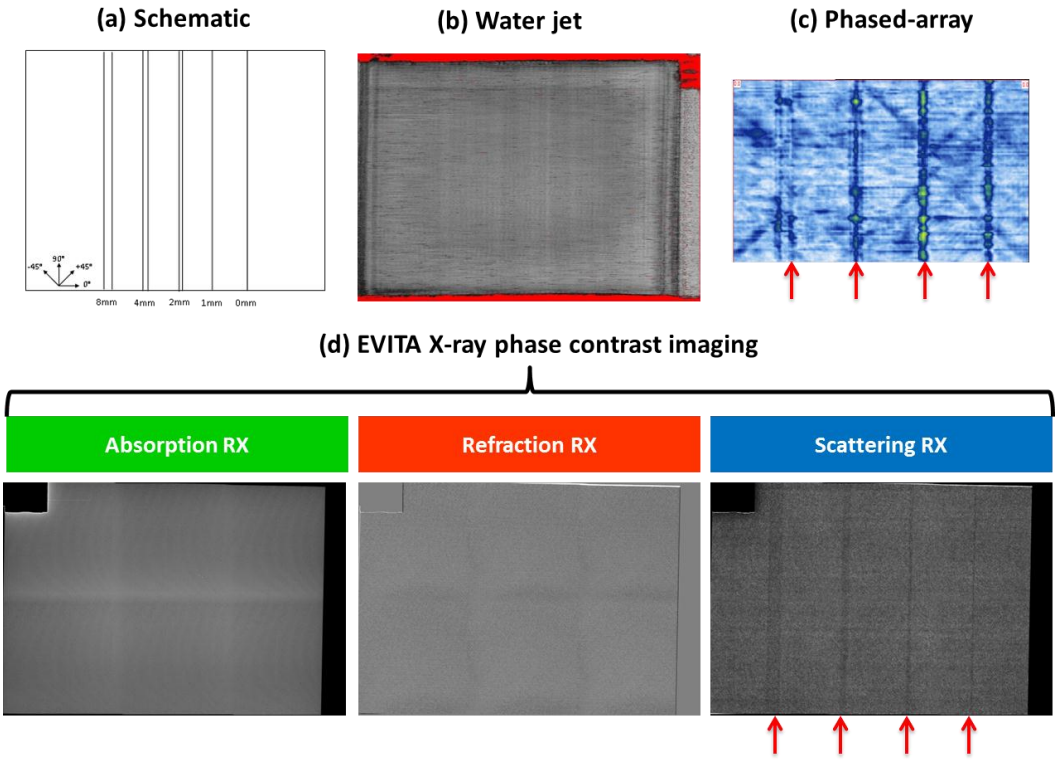

Figure 3. Results obtained on a coupon sample with cut fibres positioned as shown in (a). The images obtained by water jet and phase array ultrasonic are shown in (b) and (c). The absorption, refraction and scattering images obtained with the EVITA demonstrator are shown in (d).

Figure 3 shows the results of the comparison for a second sample, where an out-of-plane wrinkle was induced by adding additional plies at 90° as depicted in see Figure 4-a. The out-of-plane wrinkle can be detected in the scattering image (red arrows) using the EVITA demonstrator as well as with the water jet ultrasonic system. All other benchmarking methods were not able to detect the defects.

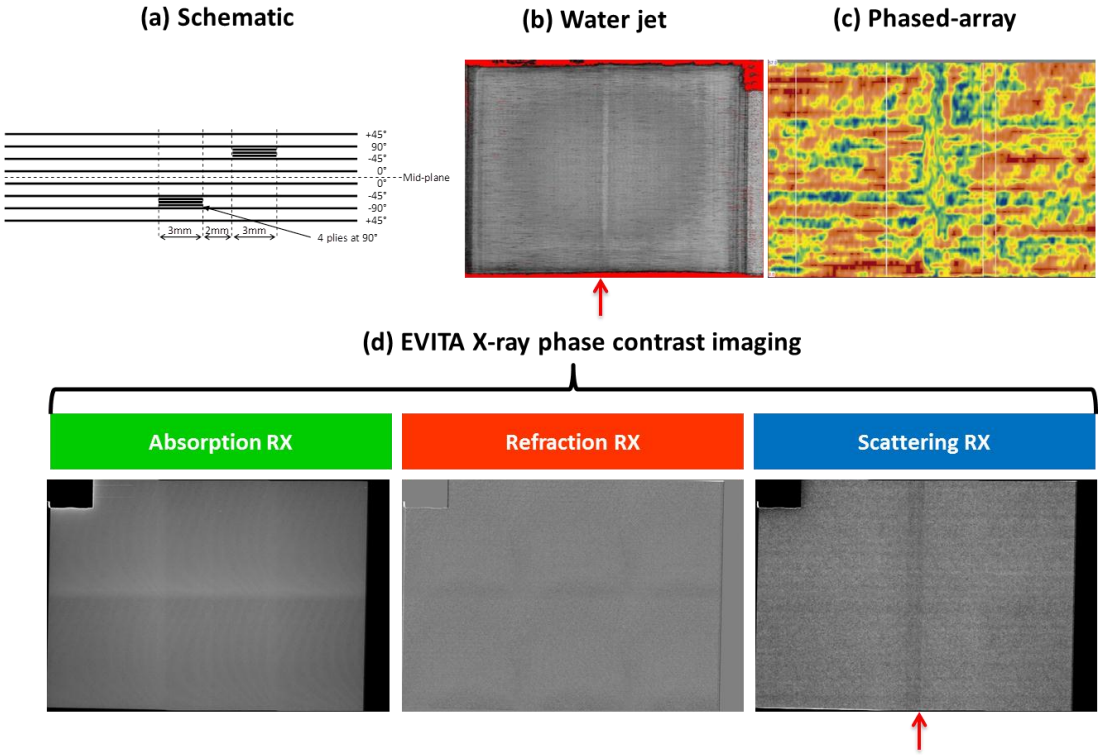

Figure 4 Results obtained on a coupon sample with an out-of-plane wrinkle induced by the layup shown in (a). The images obtained by water jet and phase array ultrasonic are shown in (b) and (c). The absorption, refraction and scattering images obtained with the EVITA demonstrator are shown in (d).

4. Conclusion

The EVITA demonstrator was presented and its performance was illustrated using two coupon samples with two types of artificial flaws: fiber cut and out-of-plane wrinkle. The flaws could be detected by the EVITA demonstrator with a comparably fast exposure time. No other NDI method used for the benchmarking was able to detect both flaws. The images obtained still display some artefacts which penalize the sensitivity of the method. However, new algorithms are currently being developed to reduce the artefacts and improve image quality.

The introduction of this innovative methodology is expected to provide the aeronautical industry with a reliable and detailed insight of the integrity of thin and thick composite structures as well as of complex geometry ones, such as integrated closed boxes and sandwiches. By increasing the level of detectability of defects in composite structures, as well as by detecting defects invisible to standard industrial non-destructive testing methodologies, the novel method will play a major role during the whole life cycle of composite components, reducing their inspection cost and increasing their reliability.

Acknowledgments

The authors acknowledge financial support from the European Union's Seventh Framework Programme for research technological development and demonstration under grant agreement n°314735.

References

David, C. et al., 2002. Differential x-ray phase contrast imaging using a shearing interferometer. *Applied Physics Letters*, 81(17), p.3287. Available at: http://link.aip.org/link/APPLAB/v81/i17/p3287/s1&Agg=doi.

Jerjen, I. et al., 2013. Detection of stress whitening in plastics with the help of X-ray dark field imaging. *Polymer Testing*, 32(6), pp.1094–1098. Available at: http://linkinghub.elsevier.com/retrieve/pii/S014294181300127X [Accessed August 23, 2013].

Kottler, C. et al., 2012. Recent developments on X-ray phase contrast imaging technology at CSEM. *AIP Conference Proceedings*, 1466(2012), pp.18–22. Available at: http://link.aip.org/link/APCPCS/v1466/i1/p18/s1&Agg=doi [Accessed August 22, 2012].

Momose, A. et al., 2003. Demonstration of X-Ray Talbot Interferometry. *Japanese Journal of Applied Physics*, 42(Part 2, No. 7B), pp.L866–L868. Available at: http://jjap.ipap.jp/link?JJAP/42/L866/ [Accessed May 5, 2012].

Pfeiffer, F. et al., 2006. Phase retrieval and differential phase-contrast imaging with low-brilliance X-ray sources. *Nature Physics*, 2(4), pp.258–261. Available at: http://www.nature.com/doifinder/10.1038/nphys265 [Accessed March 5, 2012].

Revol, V. et al., 2013. Laminate fibre structure characterisation of carbon fibre-reinforced polymers by X-ray scatter dark field imaging with a grating interferometer. *NDT&E International*, 58, pp.64–71.

Revol, V. et al., 2010. Noise analysis of grating-based x-ray differential phase contrast imaging. *Review of Scientific Instruments*, 81(7), p.73709. Available at: http://www.ncbi.nlm.nih.gov/pubmed/20687733.

Revol, V. et al., 2012. Orientation-selective X-ray dark field imaging of ordered systems. *Journal of Applied Physics*, 112, p.114903.

Revol, V. et al., 2011. Sub-pixel porosity revealed by x-ray scatter dark field imaging. *Journal of Applied Physics*, 110(4), p.44912. Available at: http://link.aip.org/link/JAPIAU/v110/i4/p044912/s1&Agg=doi.

Weitkamp, T., Diaz, A. & David, C., 2005. X-ray phase imaging with a grating interferometer. *Optics Express*, 13(16), pp.6296 – 6304. Available at: http://www.researchgate.net/publication/26268839_X-ray_phase_imaging_with_a_grating_interferometer/file/79e4150eeb57b03b82.pdf [Accessed April 5, 2013].

Yashiro, W. et al., 2010. On the origin of visibility contrast in x-ray Talbot interferometry. *Optics Express*, 18(16), pp.16890–16901. Available at: http://www.ncbi.nlm.nih.gov/pubmed/20721081.